Local Reflex Generation for Obstacle Negotiation in Quadrupedal Locomotion

MICHELE FOCCHI ° *, VICTOR BARASUOL†, IOANNIS HAVOUTIS*, JONAS
BUCHLI+, CLAUDIO SEMINI* and DARWIN G. CALDWELL*

*Dept. of Advanced Robotics, Istituto Italiano di Tecnologia (IIT),
° E-mail: michele.focchi@iit.it, http://www.iit.it/en/advanced-robotics.html
†Federal University of Santa Catarina (UFSC),
+Agile & Dexterous Robotics Lab (ADRL), ETH Zurich

Legged robots that dynamically locomote through rough terrain need to constantly handle unpredicted collisions (e.g. foot stumbling due to an obstacle) due to the unstructured nature of the environment. If these disturbances are strong enough they can cause errors in the robot's trunk that are difficult to control with a common feedback-based controller, imposing a serious risk to the overall system stability. The impulsive nature of such disturbances demands a very short reaction time, especially in case of dynamic gaits (trot, gallop, etc.). A quick reaction becomes increasingly crucial when the robot is deprived of reliable visual feedback (e.g. smoky areas or thick vegetation) or when an accurate map of the environment is not available. In this paper we propose a *local elevator reflex* which enables the robot to reactively overcome high obstacles. The reflex is implemented and experimentally evaluated on the hydraulic quadruped - *HyQ*. We demonstrate the feasibility and effectiveness of our approach showing that the robot is able to step over a platform of $11cm$ height (14% of the leg length) without prior knowledge of the terrain.

Keywords: Reflex, Quadrupedal locomotion, Control.

1. Introduction

Natural terrain is often not level, may be slippery and provide sparse footholds. One way to approach locomotion is to perform footstep planning, assuming that a reasonable map of the environment is available. However, this approach is valid for slow locomotion and has limited applicability under rapidly changing conditions. In the latter case fast reactions are mandatory for maintaining stability. Biological studies have shown that animals use local reflexes to cope with terrain irregularities.[1] This way, animals initially retract the foot and then try swinging over the obstacle. This is

2

particularly useful in situations where the leg is obstructed by an unexpected or unperceived elevation of the terrain that causes a frontal impact, making the robot stumble.

Early implementations of reflexes in robotics date back to the 80's with Bekey's work,[2] where reflex activity consisted of relating joint motion to sensory patterns following certain rules. Park et al.[3] proposed a reflex method for a legged robot to deal with slippery surfaces. More recently a reflex behaviour has been effectively implemented for the bipedal robot *Mabel*. Mabel has been shown to step up on platforms that are as high as 12% of its leg length.[4]

In this paper we propose the implementation of a reflex strategy called the *local elevator reflex*, for the hydraulic quadruped robot HyQ[5] (Fig. 1(right)). This reflex is implemented as a kinematic modification of the reference trajectory of the foot of the swing leg. An advantage of our reflex approach is that it depends on a small set of parameters that have physical meaning and can be directly linked to the locomotion parameters. This way the robot is capable of regulating the *strength* of the reflex to the locomotion situation at hand.

2. Reflex implementation

HyQ's trotting involves periodic motion generation (ellipses) for the feet together with a controller for body posture stabilization. The feet trajectories are generated by non-linear oscillators (CPGs), as described in.[6] The following section describes the generation of the reflex trajectory $\mathbf{P}_{rfx}$ for one foot, that is added as an offset to the reference $\mathbf{P}_{ref}$ generated by the CPG. $\mathbf{P}_{rfx}$ is a function of intuitive physical parameters: the reflex duration t_{rfx}, the maximum retraction r_{max}, the desired angle of retraction θ_0 and the duration t_{ret} of the retraction impulse. These parameters can be easily expressed as a function of the gait parameters. In particular the reflex duration can be varied according to the swing phase duration while the maximum retraction can be linked to the step height (Fig. 2(left)).

The reflex trajectory is generated in a coordinate frame, the *foot frame*, that is aligned with the trunk frame (Fig. 1(left)). In this derivation we are generating trajectories that lie in the $X - Z$ plane of this frame, (where x is aligned with the direction of motion of the robot) but this can be easily extended to any orientation. The reflex can only be triggered when the leg is in the air (swing phase), when the CPG phase angle $\alpha > 90°$ (Fig. 2(left)). This is because for $\alpha < 90°$ the reflex trajectory is cancelled out by the CPG trajectory, that is at that time descending. The CPG phase
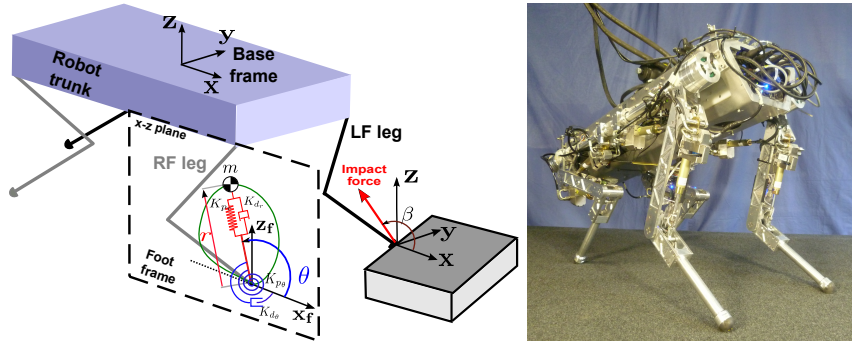
Fig. 1.   (**Left**) The reflex trajectory, if restricted to the $X - Z$ plane, can be described with radial r and angular θ coordinates. The angle β of the impact force (see left-front leg) is expressed in the $X - Z$ plane. (**Right**) Picture of the HyQ robot.

angle α represents the angle between the desired foot position vector and the x axis in the $X - Z$ plane of the foot frame. The swing phase starts at the lift-off and finishes at the touchdown event. The touchdown is detected by sensing the *ground reaction forces* (GRFs). The GRFs are estimated using the torque sensors at the joints and the Jacobian transpose of the leg kinematics. In the HyQ motion generation framework there is an adaptation mechanism which "cuts" the reference ellipses when a ground impact is detected (touchdown). This adaptation mechanism is very important to enhance robot stability when walking on rough terrain.[6] The touchdown event determines the beginning of the stance phase in which the periodic motion becomes a motion along a line parallel to the ground. This results in the leg pushing backward in the horizontal direction and thereby propelling the robot forward.

Fig. 2 (left) shows three different touchdown events and the corresponding modification of the elliptic trajectories. It also shows the areas where the reflex can be activated (ascendant semi-ellipse) and the touchdown detected (descendant semi-ellipse). These two areas should not overlap to prevent undesired activation of the reflex during stance phase. Once an impact is detected at the end-effector, during the reflex-active phase, the vector of the impact force measured at the end-effector is projected into the $X - Z$ plane to evaluate if this is a frontal impact. Then the reflex is triggered if the angle β about the x-axis (Fig. 1(right)) is such that $\beta > 120°$ or $\beta < -150°$. This range was experimentally evaluated and can be tuned according to the level of responsiveness that is desired from the robot.

After the reflex is triggered, a fast retracting motion for the foot is generated. This enables the foot to move away from the obstacle, prevents
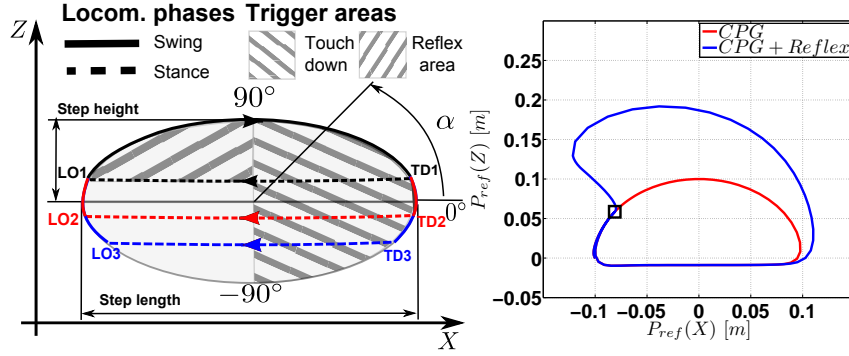
Fig. 2. (**Left**) Areas of the CPG cycle where a possible impact can trigger the limb reflex or the touchdown. α is the phase angle of the CPG trajectory. TD_i are different touch-down events that result in different stance trajectories. LO_i are the correspondent lift-off events. (**Right**) Periodic foot (clockwise) trajectory (red), and the same trajectory modified by the reflex action (blue) for overcoming a frontal obstacle. The black square indicates the collision point.

foot *trapping* and results into higher step clearance. The foot is then driven in a circular trajectory overcoming the obstacle (*swing over* motion). Since we constrain the trajectory to lie on a plane, we can implement this behavior by looking at the dynamics of a controlled unitary mass expressed in polar coordinates:

$$\ddot{\theta} + K_{d_\theta}\dot{\theta} + K_{p_\theta}\theta = 0, \qquad \ddot{r} + K_{d_r}\dot{r} + K_{p_r} = F_r(t) \qquad (1)$$

where r is the radius and θ is the angle about the X axis as depicted in Fig. 1 (left). Linear and rotational virtual springs and dampers $K_{p_r}, K_{d_r}, K_{p_\theta}, K_{d_\theta}$ attract the state variables back to the origin. Since the equations in (1) are decoupled, it is possible to define different dynamics for the radial and angular motions, respectively.

Since we initially want to have a retraction, we set an external input $F_r(t)$ only in the radial equation. This retraction force is applied only for a limited time t_{ret} (square pulse).

$$F_r(t) = \begin{cases} 0 & t < 0 \\ |Fr| & 0 > t > t_{ret} \end{cases} \qquad (2)$$

After the time t_{ret} has elapsed, the trajectory will only move towards the origin under the effect of the virtual elements. The acceleration is extracted from (1) and by double integration the reflex trajectory, $(\theta(t), r(t))$, can be obtained in polar coordinates. Before starting the integration, it is important to set the initial conditions $\theta(0) = \theta_0, r(0) = 0$ for the state variables to have the force F_r injected in the desired direction. After trans-

forming to Cartesian coordinates $(x = rcos(\theta), y = 0, z = rsin(\theta))$ the reflex trajectory $\mathbf{P}_{rfx}$ is obtained.

Fig. 2 (right) shows the effect of the addition of the reflex to the CPG trajectory. The shape of the reflex trajectory can be tuned by choosing the settling time for the angular t_{rfx_θ} and radial t_{rfx_r} dynamics. In particular these dynamics are described by the eigenvalues λ_i of the associated homogeneous linear systems.

$$\lambda^2 + K_d\lambda + K_p = 0, \qquad \lambda_{1,2} = \frac{-K_d \pm \sqrt{K_d^2 - 4K_p}}{2} \tag{3}$$

For the sake of simplicity, we decided to set $t_{rfx_r} = t_{rfx_\theta}$ by choosing the same gains K_d, K_p for θ and r. K_d is chosen to place the eigenvalues at $\lambda_i = 4.6/t_{rfx}$[7] in order to obtain the desired settling time t_{rfx}, while K_p is chosen to have λ_i as real coincident roots (critical damping):

$$K_d = 9.2/t_{rfx}, \quad K_p = K_d^2/4. \tag{4}$$

An inverse dynamics algorithm is used to compute the torque necessary to perform the reference trajectory alleviating the work of the feedback joint position controller and achieving higher control bandwidth.[8] As a matter of fact a high control bandwidth is mandatory to track the kinematic modification of the reflex because its duration will be constrained in a fraction of the time interval in which the leg is in swing phase.

Finally the value of $|Fr|$ can be set to achieve a desired maximum retraction r_{max}. To express r_{max} we investigate the analytical solution of the radial velocity $\dot{r}(t)$ finding the time instant t_{max} in which it crosses zero. We must underline that the instant where maximum retraction occurs, t_{max}, is not the instant when the pulse ends $(t = t_{ret})$ because at t_{ret} the unity mass has a non-zero instantaneous velocity that must be decelerated. The time response of the velocity to a square pulse input for a critically damped 2nd order system, is:[7]

$$\dot{r}(t) = \frac{|F_r|}{K_p}(t\lambda^2 e^{t\lambda} - \mathbf{1}_{t>t_{ret}}(t)(t - t_{ret})\lambda^2 e^{-(t-t_{ret})\lambda}) \tag{5}$$

where $\mathbf{1}(t)$ is an indicator function. After some manipulation the time instant where $\dot{r}(t_{max} = 0)$ can be found:

$$t_{max} = \frac{-t_{ret}\lambda^2 e^{t_{ret}\lambda}}{\lambda^2(1 - e^{t_{ret}\lambda})} \tag{6}$$

by putting (6) in the time response of the radius $r(t)$ we obtain the relationship:

$$r_{max} = r(t_{max}) = \frac{|F_r|}{K_p}\underbrace{(-(1+t_{max}\lambda)e^{-t_{max}\lambda} + (t_{max} - t_{ret})\lambda e^{-(t_{max}-t_{ret})\lambda})}_{A} \tag{7}$$
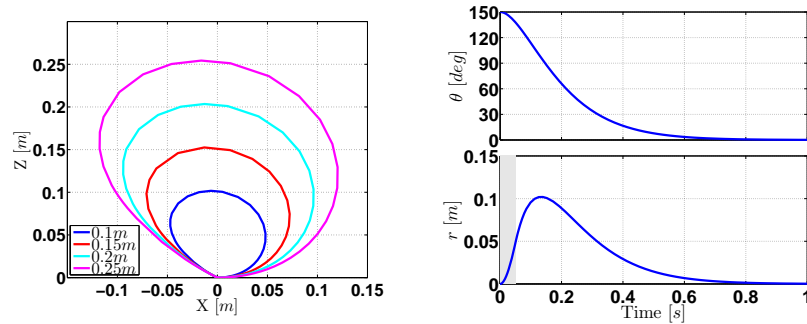
6

Fig. 3.   Simulation. (**Left**) Reflex trajectory (clockwise) in the $X - Z$ plane for different maximum retraction values. (**Right**) Time response of the polar coordinates ($t_{rfx} = 0.5s$, $r_{max} = 0.1m$ and $\theta_0 = 150°$). The shaded area highlights the interval during which the retraction impulse is acting.

Then the value of $|Fr|$ can be linked to the desired maximum retraction:

$$|\mathbf{F}_r| = \frac{r_{max}K_p}{A}. \tag{8}$$

Figure 3 (left) shows an $X - Z$ plot of the reflex trajectory for different retraction parameters, i.e. varying r_{max}. After the initial fast retraction it can be seen that the *swing over motion* is due to the dynamics of θ that, starting from θ_0, is moving towards the origin. Fig. 3 (right) shows the time response of the polar coordinates for a settling time $t_{rfx} = 0.5s$, $r_{max} = 0.1m$, and $\theta_0 = 150°$. The figure shows r and θ have the same settling time.

3. Experiments

In this section we present some experimental results that demonstrate the effectiveness of the proposed reflex algorithm, when the robot is trotting and stepping up on a $11cm$ high platform. The forward speed has been set to $0.1m/s$ while the step height has been set to $9cm$ making the reflex action necessary to overcome the step. The step length was set to $5cm$ and throughout our test we have used a cycle period frequency of $1.7Hz$. The max retraction r_{max} was set to $13cm$, and the desired angle of retraction θ_0 to $135°$. The value of the settling time t_{rfx} was computed in real-time depending on which was the value of α at the moment of the reflex trigger. In particular, smaller t_{rfx} (faster reflex trajectories) were obtained if the trigger occurred close to the apex $\alpha = 90°$. This is important for assuring the synchronization of the foot with the CPG.

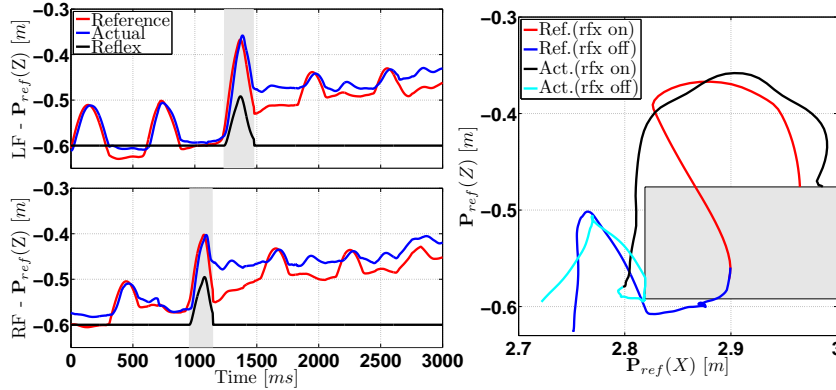Fig. 4 (left) presents the vertical components (Z) of the reference and

Fig. 4.   Experimental results. (**Left**) Step up. Vertical (Z) component of the foot position for the left-front (upper plot) and right front (lower plot) leg. Red plots are the reference trajectories while blue plots the actual ones. The reflex component of the reference trajectory (black) is offset of -0.6 m for display purposes only. The grey area shows when the reflex is active. (**Right**) Foot trajectory in the $X - Z$ plane in world coordinates when the reflex is triggered for the left-front leg.

actual foot trajectory during the step up when the robot is trotting towards the platform. The reflex is effectively triggered after the frontal impact of the feet with the platform, initially for the right-front (RF) leg and $250ms$ later for the left-front (LF) leg. Then when each foot lands on the platform a new touchdown condition is detected. The shadow area shows when the reflex is active. The foot trajectories are mapped into an inertial frame fixed to the ground at the point where the robot base is when the trot starts. This helps in estimating the real obstacle height. The small oscillations in the desired trajectory are artifacts due to the estimation errors in the robot odometry.

Fig. 4 (right) is a plot in the $X-Z$ plane that shows how the reflex modifies the trajectory of the left foot after the frontal impact with the platform. The trajectory is mapped into an inertial frame fixed with the ground. The figure shows that after the first impact the reflex was not triggered as the reference trajectory had already overpassed the apex ($\alpha = 90°$). However the reflex is successfully triggered in the following CPG cycle and the leg successfully overcomes the obstacle. This demonstrates the robustness of the proposed approach in the worst situation in which the foot hits the obstacle when it is almost at the end of the cycle ($\alpha < 90°$). The experiment has been successfully repeated on a set of 10 trials, 5 of them with an obstacle height of 8 cm and a CPG step height of 7 cm, while the other 5 with an obstacle height of 11 cm and a CPG step height of 9 cm.

8

4. Conclusions

In this paper we proposed the implementation of a *local elevator reflex*, intended to improve robot locomotion robustness when hitting high obstacles, that would otherwise cause the robot to stumble. The underlying idea is that the leg should "*give in*" instead of trying to command a trajectory that would be infeasible. As a matter of fact, if the kinematic plan is not changed, tracking the original trajectory would cause the injection of destabilizing forces. The generation of the trajectory can be linked to gait parameters that enable us to adapt the reflex shape and duration to different locomotion situations. From Fig. 4 (left) it can be seen that the cutting of the ellipses causes a reduction of the available step height when the touchdown occurs on top of the platform, this in turn reduces the step length and so the locomotion speed.

Therefore future work considers the development of a more sophisticated adaptation mechanism, that has the purpose to move the origin of the ellipse in order to adapt to the new terrain elevation and recover the locomotion capabilities.

References

1. K. Espenschied, R. Quinn, R. Beer and H. Chiel, Biologically based distributed control and local reflexes improve rough terrain locomotion in a hexapod robot *Robotics and autonomous systems* **18** (Elsevier, 1996).
2. G. Bekey and R. Tomovic, Robot control by reflex actions, in *Proc. IEEE Int. Conf. Robotics and Automation*, 1986.
3. J. H. Park and O. Kwon, Reflex control of biped robot locomotion on a slippery surface, in *Proc. ICRA Robotics and Automation IEEE Int. Conf*, 2001.
4. H.-W. Park, K. Sreenath, A. Ramezani and J. W. Grizzle, Switching control design for accommodating large step-down disturbances in bipedal robot walking, in *Proc. IEEE Int Robotics and Automation (ICRA) Conf*, 2012.
5. C. Semini, HyQ – design and development of a hydraulically actuated quadruped robot, PhD thesis, Istituto Italiano di Tecnologia (IIT)2010.
6. V. Barasuol, J. Buchli, C. Semini, M. Frigerio, E. R. De Pieri and D. G. Caldwell, A reactive controller framework for quadrupedal locomotion on challenging terrain, in *2013 IEEE International Conference on Robotics and Automation (ICRA)*, may 2013.
7. G. Franklin, *Feedback Control of Dynamic Systems*, 3rd edn. (Addison-Wesley Longman Publishing, Boston, 1993).
8. J. Buchli, M. Kalakrishnan, M. Mistry, P. Pastor and S. Schaal, Compliant quadruped locomotion over rough terrain, in *Proceedings of IEEE/RSJ International Conference on Intelligent Robots and Systems (IROS)*, 2009.